Institut "Jožef Stefan" , Ljubljana

1111 Ljubljana, Jamova 39, pp 100 / Tel: +386 61 177 3900 / Fax: +386 61 125 7074

IJS Report
IJS - DP - 7356
February 1996

The optimal detector surface of a fixed target RICH with a tilted mirror

P. Križan[a,b] and M. Starič [a]

[a] *"J. Stefan" Institute, Ljubljana, Slovenia* ,

[b] *Faculty of Mathematics and Physics, University of Ljubljana, Slovenia*

Published in Nucl. Inst. and Meth., NIM A394 (1997) 27-34

The optimal detector surface of a fixed target RICH with a tilted mirror

Peter Križan and Marko Starič

January 4, 1998

Abstract

The origin of the optical error in the Čerenkov angle measurement in the case of a tilted RICH mirror geometry is described together with possible reductions of this error. It is shown that by suitably adjusting the detector form, the resulting contribution to the overall error in Čerenkov angle measurement can be made negligible.

Introduction

In a fixed target experiment such as HERA-B [1, 2] where one has to deal with intense fluxes of charged particles, special care has to be taken when designing a ring imaging Čerenkov counter. The design choices are governed by the following criteria:

- To achieve the necessary performance, a sufficient number of photons (more than 10) has to be detected for each ring image [1, 4]. This requirement fixes the length of a gas radiator to a few meters.
- A high rate capability of the photon detector requires some kind of chamber with pads, and therefore limits the resolution to a few milimeters (assuming that only digital information is read out, rather than pulse height).
- The required high resolution in the measurement of the Čerenkov angle with such a photon detector is only achievable if the focal length is kept at several meters.
- The delicacy of the photon detector with a very low detection threshold, necessary to count single photoelectrons, requires the photon detector to be kept out of the solid angle for charged particles and conversion products.

The set-up of the counter is schematically shown in Fig. 1. The spherical mirror is tilted, i.e. the center of curvature of the mirror is displaced relative to the target position, by which photons are reflected to photon detectors well outside the charged particle flux. Such a set-up has, however, one important drawback if compared to the case where the center of the spherical mirror coincides with the position of the target. It turns out [3] that in the latter case the spherical aberration is negligible if the photon detector is positioned on the focal sphere with a radius that is very close to half the radius of curvature of the mirror. In the case of a tilted mirror, however, the angles of incidence of photons upon the mirror surface are large, typically of the order of the tilt angle. As a result, parallel photons will not intercept the photon detector surface at the same point, and the Čerenkov rings will get smeared. For tilts of the order of

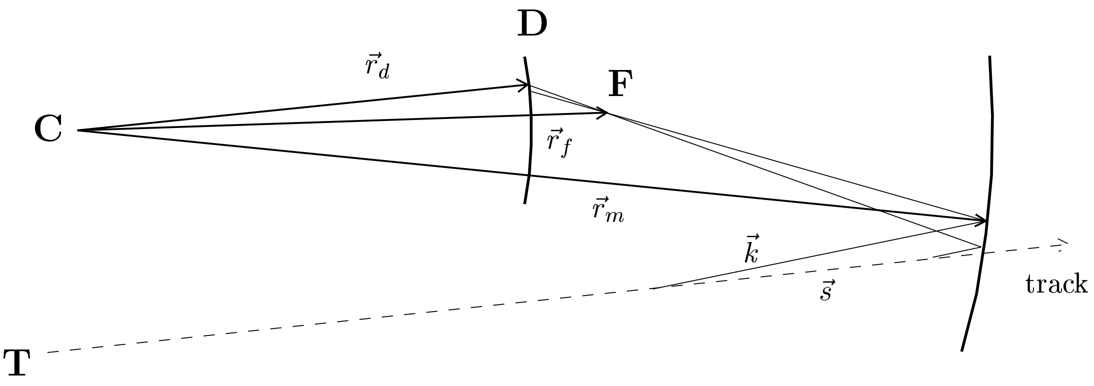

Figure 1: *The set up of the RICH optical system: tracks originate in the target T and produce Čerenkov photons along the path in the radiator. The photons, in turn, are reflected at the mirror surface with center of curvature at C, and hit the detector surface D.*

10^0 the resulting error in the measurement of the Čerenkov angle becomes of the same order as the dominant contributions to the error, the photon detection precision and chromatic aberration.

While an excellent survey of various error sources in Čerenkov angle measurement can be found in [3], it is the subject of this paper to discuss the optical error and its reduction for the special case of a RICH with a tilted mirror. We shall in particular discuss the optimization of the photon detector surface in the case of the HERA-B RICH.

The focus

Let $\vec{r}_m$ be a point on the mirror surface with radius of curvature equal to r_m, and let $\vec{n}_m$ denote the corresponding unit vector, $\vec{n}_m = \vec{r}_m / r_m$ (Fig. 1). For a photon with directional vector $\vec{k}$ hitting the mirror surface at $\vec{r}_m$, it is straightforward to show that it intercepts the spherical detector surface of radius r_d at the point

$$\vec{r}_d = \vec{r}_m + \lambda \vec{k}_R, \tag{1}$$

where $\vec{k}_R$ denotes the reflected photon direction,

$$\vec{k}_R = \vec{k} - 2(\vec{k} \cdot \vec{n}_m)\vec{n}_m, \tag{2}$$

and

$$\lambda = r_m[(\vec{k} \cdot \vec{n}_m) - \sqrt{(\vec{k} \cdot \vec{n}_m)^2 - 1 + (\frac{r_d}{r_m})^2}]. \tag{3}$$

We shall now turn our attention to the question of what is meant by focus in the case of a RICH. The optical system of a RICH counter should image to a point on the detector surface parallel photons that have been emitted in the direction $\vec{k}$ at various points along the track. The focal point is thus determined by requiring a vanishing variation of $\vec{r}_d$ if the point where the photon hits the mirror surface changes by $\delta\vec{n}_m$, while the photon direction $\vec{k}$ is kept constant. The vector $\delta\vec{n}_m$, in turn, lies in the plane span by the track direction $\vec{s}$ and by the photon direction $\vec{k}$. In the case of a spherical mirror, it is further constrained by

$$\delta\vec{n}_m \cdot \vec{n}_m = 0, \tag{4}$$

and is therefore proportional to

$$\delta\vec{n}_m \propto \vec{k}(\vec{s}\cdot\vec{n}_m) - \vec{s}(\vec{k}\cdot\vec{n}_m). \tag{5}$$

The variation of expression 1 with respect to $\vec{n}_m$ yields

$$\delta\vec{r}_d = r_m[A\delta\vec{n}_m + (\delta\vec{n}_m\cdot\vec{k})(B\vec{k} + C\vec{n}_m)] \tag{6}$$

with

$$\begin{aligned}
A = 1 \quad &- \quad 2(\vec{k}\cdot\vec{n}_m)[(\vec{k}\cdot\vec{n}_m) - \\
&\quad -\sqrt{(\vec{k}\cdot\vec{n}_m)^2 - 1 + (\frac{r_d}{r_m})^2}],\\
B = 1 \quad &- \quad \frac{(\vec{k}\cdot\vec{n}_m)}{\sqrt{(\vec{k}\cdot\vec{n}_m)^2 - 1 + (\frac{r_d}{r_m})^2}},\\
C = 2 \quad &[\quad -2(\vec{k}\cdot\vec{n}_m) + \sqrt{(\vec{k}\cdot\vec{n}_m)^2 - 1 + (\frac{r_d}{r_m})^2}\\
&+ \quad \frac{(\vec{k}\cdot\vec{n}_m)^2}{\sqrt{(\vec{k}\cdot\vec{n}_m)^2 - 1 + (\frac{r_d}{r_m})^2}}].
\end{aligned} \tag{7}$$

Clearly A, B and C depend on r_d. The focal surface is then determined by adjusting r_d in such a way that a specific projection of $\delta\vec{r}_d$ onto the detector surface vanishes. From Fig. 1 we see, that of the projections onto the three simple vectors that are at our disposal, $\vec{k}$, $\vec{n}_m$ and $\delta\vec{n}_m$, the latter,

$$\delta\vec{n}_m\cdot\delta\vec{r}_d = r_m[A(\delta\vec{n}_m)^2 + B(\delta\vec{n}_m\cdot\vec{k})^2], \tag{8}$$

is the relevant one for the size of the spot on the detector surface, since $\delta\vec{n}_m$ is closest to pointing along the radial direction of the Čerenkov circle on the detector surface. If Eq. 8 is required to vanish, we arrive at the expression for r_f, the distance of the focal surface from the center of curvature of the mirror,

$$r_f = \frac{r_m}{2}\frac{\sqrt{1+2g}}{(\vec{k}\cdot\vec{n}_m)} \tag{9}$$

where

$$g = \frac{(\cos\theta_t - (\vec{k}\cdot\vec{n}_m)\cos\vartheta_C)^2}{\cos^2\theta_t - 2(\vec{k}\cdot\vec{n}_m)\cos\vartheta_C\cos\theta_t + (\vec{k}\cdot\vec{n}_m)^2},$$

ϑ_C is the Čerenkov angle and θ_t is the angle of incidence of the track upon the mirror surface, $\cos\theta_t = \vec{s}\cdot\vec{n}_m$. In Fig. 2, r_f is plotted for three mirror tilts, 6^0, 9^0 and 15^0, for the C_4F_{10} gas radiator ($\vartheta_C = 0.0556$ for $\beta = 1$ particles).

It is worth noting that if we project $\delta\vec{r}_d$ onto $\vec{n}_m$ or $\vec{k}$, and require the variation to vanish, the corresponding expression for the distance of the focal surface from the center of curvature of the mirror is

$$r_f = \frac{r_m}{2}\sqrt{4 - 3(\vec{k}\cdot\vec{n}_m)^2}. \tag{10}$$

Clearly, Eq. 10 coincides with Eq. 9 when $\vec{k}$, $\vec{n}_m$ and $\delta\vec{n}_m$ are coplanar, and can be used as a simple approximation to the proper but somewhat more complicated Eq. 9.

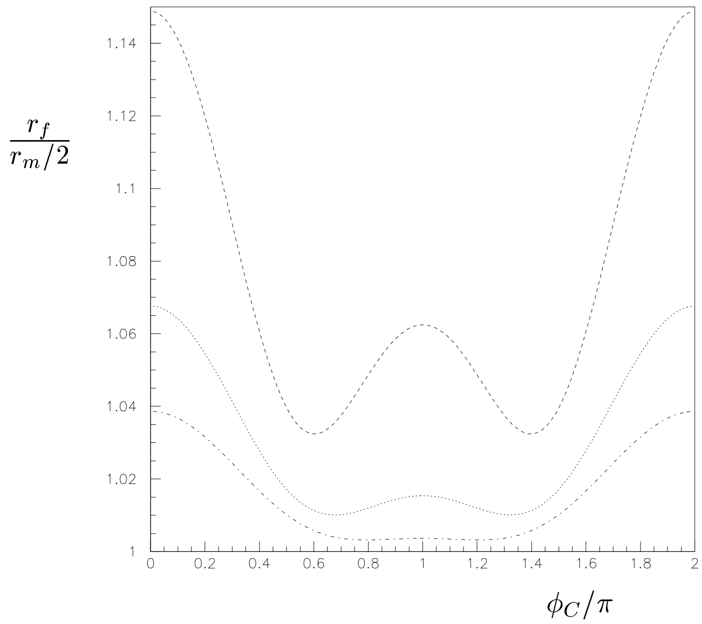

Figure 2: *The focal surface position r_f relative to the naive $r_d = r_m/2$ sphere as a function of ϕ_C, the photon azimuthal angle with respect to the track direction. The three curves shown correspond to different angles of incidence of the track upon the mirror surface:* 15^0 *(dashed),* 9^0 *(dotted) and* 6^0 *(dash-dotted). The Čerenkov angle is 0.0556.*

As already pointed out in [3], there is a small correction relative to the naive $r_m/2$ detector position even if the target coincides with the mirror center of curvature and there is no magnetic field, so that $\theta_t = 0$. If $(\vec{k} \cdot \vec{n}_m)$ is calculated for photons emitted in the middle of a gaseous radiator that is assumed to fill up the space between the mirror and the photon detector, and if we take into account that the Čerenkov angle for a gas radiator is small, Eq. 10 yields $r_f = \frac{r_m}{2}(1 + \frac{27}{32}\sin^2\vartheta_C)$, in agreement with the corresponding result derived in Ref. [3]. For the C_4F_{10} radiator and $r_m = 11.5$ m this would mean a shift of 15 mm relative to the $r_m/2$ sphere.

The optical error

We first note that for photons with a fixed $\vec{k}$, the entry points on the mirror surface are uniformly distributed over a distance $L\vartheta_C$, where L is the length of radiator. The spread Δ on the photon detector surface, i.e. the width of the ring, is then determined by relating the two triangles (Fig. 1) with a common top in the focus F. Δ is thus approximately equal to

$$\Delta \doteq \frac{|r_f - r_d|}{r_m - r_f} L\vartheta_C, \tag{11}$$

where r_d is the local radius of the detector, and r_f is given by Eq. 9. From it the RMS error in the Čerenkov angle can be calculated,

$$\sigma_{\vartheta_C} = \frac{1}{\sqrt{12}}\frac{\Delta}{r_m/2}, \tag{12}$$

and is shown in Fig. 3 for two cases of detector surfaces.

Let us calculate this error for the case of the photon detector kept at the naive focal surface, i.e. on a sphere at half the mirror radius of curvature, $r_d = r_m/2$. The corresponding RMS error reaches its maximal value when the photon angle of incidence

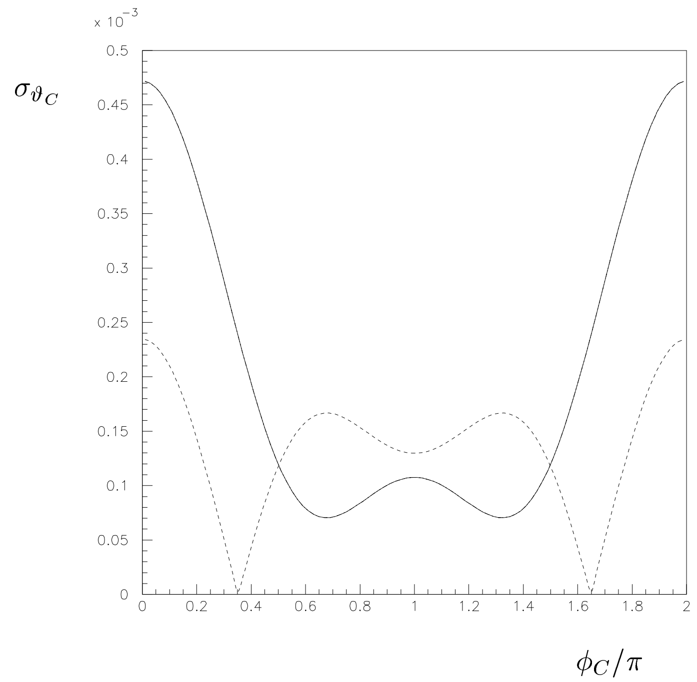

Figure 3: *The RMS error in the reconstructed Čerenkov angle for two detector configurations, spheres with radius $r_m/2$ (full) and $1.034(r_m/2)$ (dashed), shown as a function of the azimuthal angle of Čerenkov photons. The figure is plotted for a mirror with $r_m = 11.5$ m, tilted by 9^0, and a Čerenkov angle of 0.0556.*

upon the mirror surface is largest

$$\sigma_{\vartheta_C}^{max} = \frac{\sqrt{3}}{4}\frac{(\theta_t + \vartheta_C)^2 L\vartheta_C}{r_m}, \tag{13}$$

where we have assumed that θ_t, the angle by which the mirror is tilted with respect to the tracks, is small. As expected, the optical error due to spherical aberration depends quadratically on the mirror tilt angle. It is worth noting that in the HERA-B case ($\theta_t = 9^0$, $\vartheta_C = 0.0556$, $L = 2.5$ m) this error would correspond to an error caused by a photon detector pad granularity of 5 mm and therefore cannot be neglected if compared to the actual pad size of 7.5 mm.

Compensation of the error

One could fully compensate for this optical error by designing the photon detector in such a way that the chambers are aligned along the focal surface, $r_d = r_f$. It is easy to see, however, that in the Eq. 9 the scalar product $(\vec{k}\cdot\vec{n}_m)$ varies considerably with ϕ_C, the azimuthal angle of the Čerenkov photon around the track direction, $(\vec{k}\cdot\vec{n}_m) = \cos\theta_t\cos\vartheta_C - \sin\theta_t\sin\vartheta_C\cos\phi_C$, where ϕ_C is counted from the plane span by $\vec{s}$ and $\vec{n}_m$. The corresponding variation of the focal plane position is shown in Fig. 2. As the difference between extreme values of r_f is quite large (e.g. 5% of $r_m/2$ in the case of a 9^0 tilt, corresponding to about 30 cm across a circle of 68 cm in diameter in the case of HERA-B), it is only possible to partially compensate for the departure of the focal surface from a smooth detector surface.

Moreover, when optimizing the detector form one has to take into account that on each detector segment photons are detected that originate from Čerenkov circles with centers around the point in question, each of them requiring a specific value of r_f. At a given point of the detector surface far from boundaries of the acceptance, the optimal value of r_f would roughly correspond to a value of r_f averaged over ϕ_C

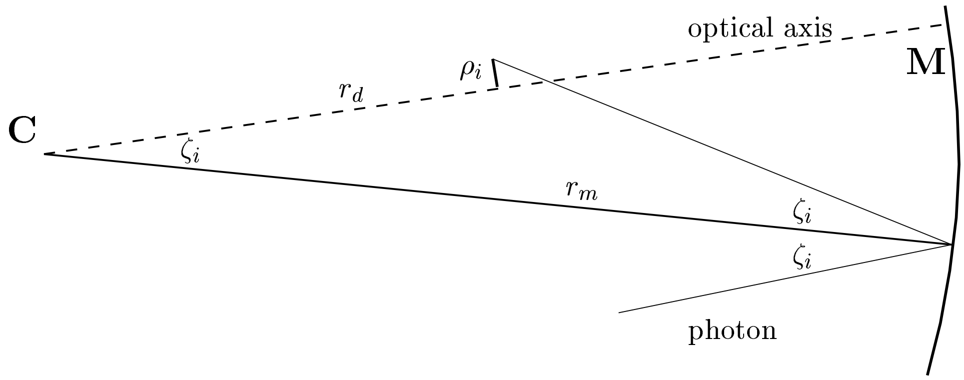

Figure 4: *The definition of ρ_i: the distance between the intersections of the optical axis and reflected photon direction with the tangential plane at r_d.*

(Fig. 2). In the case of the 9^0 mirror tilt this would, for example, correspond to a value of $r_f = 1.034 \cdot (r_m/2)$, i.e. to an increase in the detector sphere radius by about 20 cm for $r_m = 11.5$ m. The averaging of r_f at the edges of acceptance corresponds to leaving out parts of the interval in ϕ_C around 0 or π, thus restricting the average value to the two extreme values in Fig. 2 (corresponding to shifts of roughly 30 cm or 10 cm, respectively).

A realistic optimization clearly has to take into account the finite geometrical acceptance of the tracking system and of the mirror. A simulation program was written that generates photons from charged tracks originating in the target. For parallel photons that hit a given detector segment, the average focal surface distance from the mirror center of curvature was adjusted in order to minimize the spot size. This was determined in the following way. For each photon i emitted within a given solid angle region (10 mrad in the azimuthal angle and 10 mrad in the declination) the departure ρ_i of the intersection of the reflected photon with the detector surface at r_d, from the intersection of the optical axis corresponding to the incident photon with the detector surface (Fig. 4). Minimizing the spot size corresponds to finding the value of r_d for which the spread in ρ,

$$\sigma_\rho^2 = \frac{1}{N}\sum_{i=1}^{N}\rho_i^2 - \frac{1}{N^2}(\sum_{i=1}^{N}\rho_i)^2 \tag{14}$$

is minimal. By making use of Fig. 4 we find the relation between ρ_i, r_d and ζ_i,

$$\frac{r_m}{2\cos\zeta_i} - r_d = \frac{\rho_i}{\tan 2\zeta_i} \tag{15}$$

and finally arrive at the expression for r_d,

$$r_d = \frac{N\sum r_i \tan^2 2\zeta_i - \sum r_i \tan 2\zeta_i \sum \tan 2\zeta_i}{N\sum \tan^2 2\zeta_i - (\sum \tan 2\zeta_i)^2}, \tag{16}$$

where in the equations above all of the sums run over all N photons that were emitted in the same solid angle region (10 mrad times 10 mrad).

For the case of a 9^0 mirror tilt and C_4F_{10} gas radiator, the resulting optimized detector surface is shown in Fig. 5 as a function of two angles, defined as follows. The declination corresponds to an angle in the plane in which the mirror is tilted,

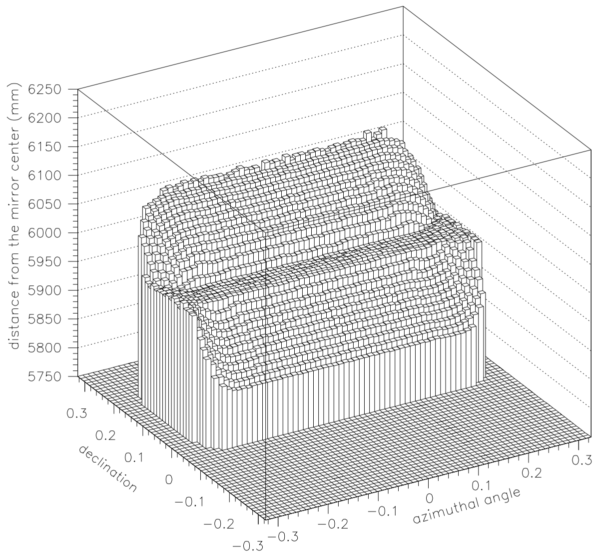

Figure 5: *The surface of least spherical aberration: the distance (in mm) of the best focus from the center of curvature of the mirror as a function of two angles, defined in the text. The radius of curvature equals to 11.5 m, the radiator gas is* C_4F_{10} *with* $\vartheta_C = 0.0556$*. Note that the naive focal surface, the* $r_m/2$ *sphere, corresponds to the base plane.*

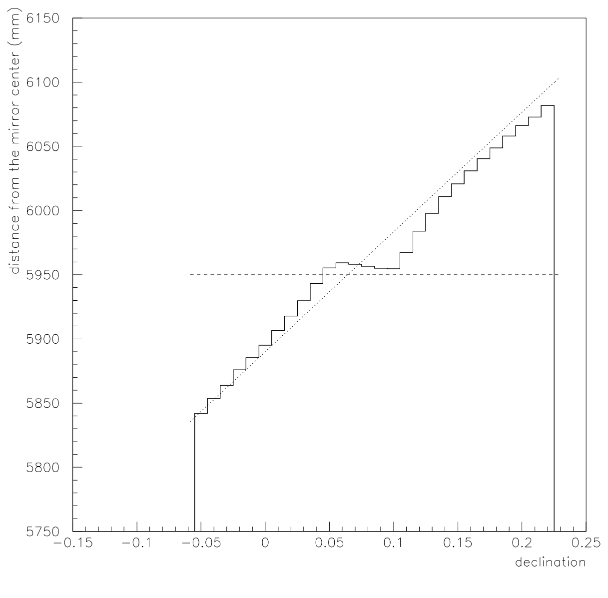

Figure 6: *The distance of the best focus from the center of curvature of the mirror as a function of the declination. Also shown are the two approximations (dotted and dash-dotted curves), discussed in the text.*

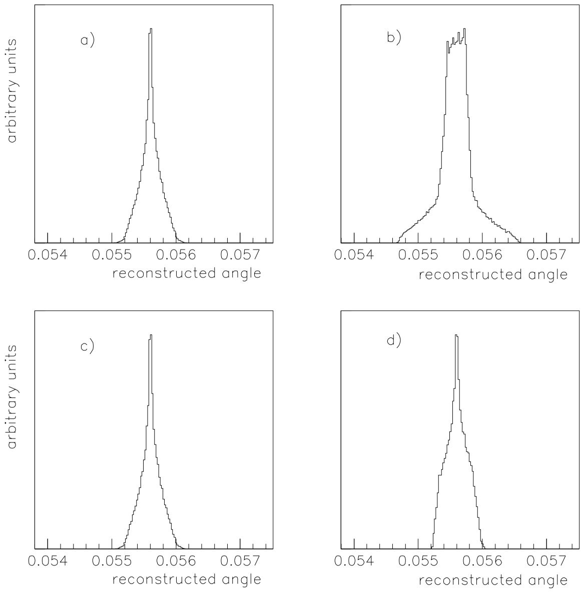

Figure 7: *The distribution of the reconstructed Čerenkov angles for four detector configurations: the best focus (a), the naive $r_m/2$ sphere (b), and the two approximations, spheres with (c) and without (d) a displaced center of curvature.*

while the azimuthal angle is counted perpendicularly to this plane, and the origin of the system coincides with the center of the Čerenkov circle of a track along the beam direction. The boundaries of the surface are set by the solid angle acceptance of the spectrometer. Both basic features of the optimal surface, the plateau in the middle and the two extreme values at the edges of acceptance, are in good agreement with expectations, discussed at the beginning of this section. For comparison, the optimized detector surface for the argon gas radiator (with a Čerenkov angle of $\vartheta_C = 0.025$) would have a much wider plateau due to the smaller diameter of Čerenkov circles [5].

A realistic detector surface

The optimized detector surface shown in Figs. 5 and 6 is not very practical. We have therefore tried to approximate by two types of spheres. In the first case the center of the sphere of radius $r_m/2 + 20$ cm coincided with the mirror center of curvature such that the surface fitted the plateau in Figs. 5 and 6. In the second case the sphere center was shifted so that the detector form fitted the slopes of the optimal detector surface Fig. 6, and its radius was set to $r_m/2 + 15$ cm.

To check the optical error in case of various detector surfaces we have generated $\beta = 1$ charged tracks uniformly over the acceptance solid angle. We have then generated for each track Čerenkov photons along the track path in the radiator. By a reconstruction algorithm that is described in Appendix A, we have calculated Čerenkov angle for each hit, assuming that the emission point was half way between the radiator entrance and mirror surface. No other contributions to the resolution were considered.

In Fig. 7 we plot the resulting distribution of Čerenkov angles for four detector

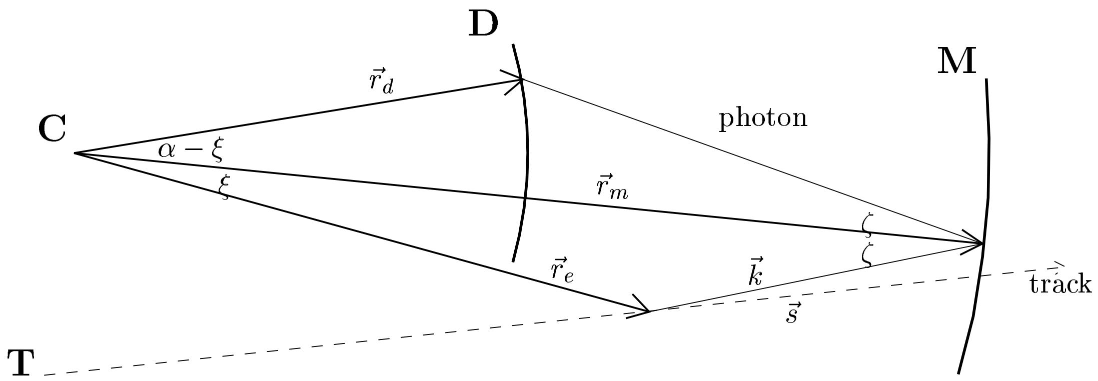

Figure 8: *Reconstruction of the Čerenkov angle: definition of the angles. Note that all vectors, except $\vec{s}$, lie in the same plane.*

configurations: a spherical detector at the naive focal surface $r_m/2$ away from the center of the mirror sphere, the best focus detector as shown in Fig. 5, and the two approximations, spheres with and without a displaced center of curvature (Fig. 6). The RMS widths of the corresponding distributions are 0.160 mrad, 0.289 mrad, 0.160 mrad and 0.167 mrad, respectively.

The spherical surface with the displaced center is closest to the optimal detector surface and results in a distribution of reconstructed Čerenkov angles that approximates very nearly the distribution in case of the optimal surface. For such a detector form, the optical error becomes small, and for the HERA-B RICH it is negligible compared to the two main sources, the granularity of the photon detector (0.40 mrad RMS) and dispersion (0.38 mrad RMS).

In the final detector design the spherical surface clearly has to be replaced by planar modules. If their size is not too large, the departures from this optimal surface can be made small enough (e.g. few milimeters for modules of size 30 cm x 30 cm), so that it causes a negligible increase in the error.

Appendix

For the sake of completeness let us derive the Čerenkov angle from the measured hit coordinate and assumed emission point position. The interested reader is referred to the general treatment of the problem in ref. [3].

Let $\vec{s}$ denote the direction of the track, $\vec{r}_e$ be the point of emission of the photon, and $\vec{r}_d$ be the hit coordinate (Fig. 8). As before, denote by $\vec{r}_m$ the point on the mirror surface, where the photon hits the mirror. To calculate the cosine of the Čerenkov angle,

$$\cos\vartheta_C = (\vec{r}_m - \vec{r}_e) \cdot \vec{s}/(|\vec{r}_m - \vec{r}_e|), \tag{17}$$

we have to determine the components of the vector $\vec{r}_m$.

From the law of reflection it is clear that the two triangles in Fig. 8 lie in the same plane, and are related by

$$\begin{aligned} \frac{\sin(\xi+\zeta)}{r_m} &= \frac{\sin\zeta}{r_e}, \\ \frac{\sin(\alpha-\xi+\zeta)}{r_m} &= \frac{\sin\zeta}{r_d}. \end{aligned} \tag{18}$$

In this system of trigonometric equations there are two unknown angles, ξ and ζ, while α, the angle between $\vec{r}_e$ and $\vec{r}_d$, is given by the relation $\cos\alpha = (\vec{r}_e \cdot \vec{r}_d)/(r_e r_d)$. The system can be solved numerically by iteration that converges very rapidly.

Once the two angles ζ and ξ have been determined, we can proceed with the calculation of components of the vector $\vec{r}_m$. Due to the law of reflection, vectors $\vec{r}_m$, $\vec{r}_e$ and $\vec{r}_d$ lie in the same plane, so that $\vec{r}_m$ can be written as

$$\vec{r}_m = \mu_e \vec{r}_e + \mu_d \vec{r}_d. \tag{19}$$

The projection of the above equation onto vectors $\vec{r}_e$ and $\vec{r}_d$ yields a set of linear equations for the coefficients μ_e and μ_d,

$$\begin{aligned} \mu_e r_e + \mu_d r_d \cos\alpha &= r_m \cos\xi, \\ \mu_e r_e \cos\alpha + \mu_d r_d &= r_m \cos(\alpha - \xi). \end{aligned} \tag{20}$$

After a straightforward derivation we arrive at the two coefficients,

$$\begin{aligned} \mu_e &= \frac{r_m}{r_e} \frac{\sin(\alpha - \xi)}{\sin\alpha}, \\ \mu_d &= \frac{r_m}{r_d} \frac{\sin\xi}{\sin\alpha}, \end{aligned} \tag{21}$$

which then allows us to calculate the Čerenkov angle by combining Eqs. 17 and 19.

References

[1] T. Lohse et al., Proposal for HERA-B, DESY-PRC 94/02, May 1994

[2] P. Križan, R. Mankel, D. Ressing, S. Shuvalov, M. Spahn, Nucl. Instr. Meth. **A351**(1994)111

[3] T. Ypsilantis, J. Seguinot, Nucl. Instr. Meth. **A343**(1994)30

[4] G. Močnik, HERA-B Note 94-029, 1994; G. Močnik, Diplomsko delo - Diploma Thesis, University of Ljubljana, 1995.

[5] P. Križan and M. Starič, IJS-DP-7053, Ljubljana 1995; HERA-B Note 95-131, DESY, Hamburg 1995.